

Multi-objective genetic algorithm applied to spectroscopic ellipsometry of organic-inorganic hybrid planar waveguides

Vasco R. Fernandes,^{1,3} Carlos M. S. Vicente,^{1,3} Naoya Wada,⁴ Paulo S. André,^{1,3,*} and Rute A. S. Ferreira^{1,2,5}

¹ Department of Physics, University of Aveiro, Campus de Santiago, 3810-193 Aveiro, Portugal

² CICECO, University of Aveiro, Campus de Santiago, 3810-193 Aveiro, Portugal

³ Instituto de Telecomunicações, Universidade de Aveiro, Campus de Santiago, 3810-193 Aveiro, Portugal

⁴ National Institute of Information and Communications Technology (NICT), Tokyo, Japan.

⁵ rferreira@ua.pt

*pandre@av.it.pt

Abstract: The applicability of multi-objective optimization to ellipsometric data analysis is presented and a method to handle complex ellipsometric problems such as multi sample or multi angle analysis using multi-objective optimization is described. The performance of a multi-objective genetic algorithm (MOGA) is tested against a single objective common genetic algorithm (CGA). The procedure is applied to the characterization (refractive index and thickness) of planar waveguides intended for the production of optical components prepared sol-gel derived organic-inorganic hybrids, so-called di-ureasils, modified with zirconium tetrapropoxide, $\text{Zr(OPr}^n)_4$ deposited on silica on silicon substrates. The results show that for the same initial conditions, MOGA performs better than the CGA, showing a higher success rate in the task of finding the best final solution.

©2010 Optical Society of America

OCIS codes: (120.2130) Ellipsometry and polarimetry; (310.6860) Thin films, optical properties; 230.7390 Waveguides, planar

References and links

1. P. Drude, "Über die Gesetze der Reflexion und Brechung des Lichtes an der Grenze absorbierender Kristalle," *Annalen der Physik* **32**, 584–625 (1887).
2. A. Rothen, "The Ellipsometer, an Apparatus to Measure Thicknesses of Thin Surface Films," *Rev. Sci. Instrum.* **16**(2), 26–30 (1945).
3. M. Land, J. J. Sidorowich, and R. K. Belew, "Using Genetic Algorithms with Local Search for Thin Film Metrology," in *Proceedings of the Seventh International Conference on Genetic Algorithms*, T. Bäck, ed., (Morgan Kaufmann Publishers, Inc, 1997), pp. 537–544.
4. O. Polgár, M. Fried, T. Lohner, and I. Bársony, "Comparison of algorithms used for evaluation of ellipsometric measurements - Random search, genetic algorithms, simulated annealing and hill climbing graph-searches," *Surf. Sci.* **457**(1-2), 157–177 (2000).
5. A. Kudla, "Application of the genetic algorithms in spectroscopic ellipsometry," *Thin Solid Films* **455–456**, 804–808 (2004).
6. O. Polgár, P. Petrik, T. Lohner, and M. Fried, "Evaluation strategies for multi-layer, multi-material ellipsometric measurements," *Appl. Surf. Sci.* **253**(1), 57–64 (2006).
7. B. Neto, A. L. J. Teixeira, N. Wada, and P. S. André, "Efficient use of hybrid Genetic Algorithms in the gain optimization of distributed Raman amplifiers," *Opt. Express* **15**(26), 17520–17528 (2007).
8. R. A. S. Ferreira, C. M. S. Vicente, V. Fernandes, A. G. Macedo, E. Pecoraro, R. Nogueira, P. S. André, P. V. S. Marques, and L. D. Carlos, "Organic-inorganic hybrids for the new generation of optical networks," in *Proc. of International Conference on Transparent Optical Networks (ICTON 2009)* (IEEE, S. Miguel (Portugal), July, 2009), pp. Tu.B4.2–1.
9. C. Molina, R. A. Sá Ferreira, L. D. Carlos, R. R. Gonçalves, S. J. L. Ribeiro, Y. Messaddeq, P. J. Moreira, O. Soppera, A. P. Leite, P. S. V. Marques, and V. de Zea Bermudez, "Planar and UV written channel optical waveguides prepared with siloxane-poly(oxyethylene)-zirconia organic-inorganic hybrids. Structure and optical properties," *J. Mater. Chem.* **15**(35-36), 3937–3945 (2005).
10. D. C. Oliveira, A. G. Macedo, N. J. O. Silva, C. Molina, R. A. Sá. Ferreira, P. S. Andre, K. Dahmouche, V. de Zea Bermudez, Y. Messaddeq, S. J. L. Ribeiro, and L. D. Carlos, "Photopatternable di-ureasil-zirconium

- oxocluster organic-inorganic hybrids as cost effective integrated optical substrates," *Chem. Mater.* **20**(11), 3696–3705 (2008).
11. E. Pecoraro, S. García-Revilla, R. A. S. Ferreira, R. Balda, L. D. Carlos, and J. Fernández, "Real time random laser properties of Rhodamine-doped di-ureasil hybrids," *Opt. Express* **18**(7), 7470–7478 (2010).
 12. O. Acher, E. Bigan, and B. Dré villon, "Improvements of phase-modulated ellipsometry," *Rev. Sci. Instrum.* **60**(1), 65–77 (1989).
 13. A. Konak, D. W. Coit, and A. E. Smith, "Multi-objective optimization using genetic algorithms: A tutorial," *Reliab. Eng. Syst. Saf.* **91**(9), 992–1007 (2006).
 14. K. Deb, A. Pratap, S. Agarwal, and T. Meyarivan, "A fast and elitist multiobjective genetic algorithm: NSGA-II," *IEEE Trans. Evol. Comput.* **6**(2), 182–197 (2002).
 15. K. Deb, and M. Goyal, "A Combined Genetic Adaptive Search (GeneAS) for Engineering Design," *Comput. Sci. Inform.*, **26**, 30–45 (1996).
 16. E. D. Palik, *Handbook of Optical Constants of Solids* (Academic Press, New York, 1998).
 17. C. M. S. Vicente, E. Pecoraro, R. A. S. Ferreira, P. S. André, R. Nogueira, Y. Messaddeq, S. J. L. Ribeiro, and L. D. Carlos, "Waveguides and gratings fabrication in zirconium-based organic/inorganic hybrids," *J. Sol-Gel Sci. Technol.* **48**(1-2), 80–85 (2008).
-

1. Introduction

Spectroscopic ellipsometry is nowadays a standard optical technique for thin films characterization. The physical background, first introduced in 1887 [1], and latter termed as ellipsometry by Alexandre Rothen [2] became relevant with the availability of computers due to the lack of inverse expressions to direct extract the optical parameters and thickness of multilayer structures, such as thin films. Traditionally gradient based minimization algorithms, such as Levenberg-Marquardt, a nonlinear least squares local optimizer (LO), are used as optimization tools in ellipsometric problems. However, similarly to other local optimizers, the performance of the Levenberg-Marquardt algorithm depends on the complexity of the search space, the number of variables and a good starting point, being possible that the optimization would be trapped in a local minimum. The use of a composite approach, with a global optimizer, like genetic algorithms (GA's), combined with a local optimizer is advantageous in complex problems due to the improved search power and better capacity to avoid local minima [3–7]. The GA is used to find the vicinity of the global minimum rather than the minimum itself. The remaining search is performed by the LO method. Therefore, making simultaneous use of the two methods combines in a single step the convergence and search capability of GA and the high accuracy of the LO.

The usage of enhanced multi-objective algorithm is helpful in spectroscopic ellipsometry data analysis because it enables the combination of measurements from multiple samples, complex multilayer structures, different incidence angles and/or the usage of external reflectance (or transmittance) data. This can enhance the information content about a set of samples and thus be beneficial to reduce ambiguity, improving the results confidence. Usually, this type of analysis is accomplished using the conventional optimization techniques with one objective function, which suffers from constraints associated with local optimization.

In this context, spectroscopic ellipsometry multi-sample analysis will be used to calculate the refractive index and thickness values of sol-gel derived planar waveguides of methacrylic acid (McOH) modified zirconium tetrapropoxide, $Zr(OPr^i)_4$, classed as di-ureasil-zirconium oxo-cluster hybrid (di-ureasils-Zr-OMc). Di-ureasils-Zr-OMc hybrids have been used in the last years as integrated optics substrates for Y-power splitters, optical filters, and Fabry-Perot cavities [8–10]. In this work we proposed an approach based on a multi-objective genetic algorithm (MOGA) simultaneously with a single objective local optimization algorithm applied to spectroscopic ellipsometry, with the subjacent advantage of improving the uniqueness and confidence in the final solutions and reducing the computation time require to solve the problem. As far as we know, this approach to solve the complex problems associated with spectroscopic ellipsometry is a novelty.

2. Experimental

2.1 Sample preparation

The reagents O, O'-Bis(2-aminopropyl) polypropylene glycol-block-polyethylene glycolblock-polypropylene glycol (Fluka), commercially known as Jeffamine-ED600®, average molecular weight 600 g.mol^{-1} , 3-isocyanatepropyltriethoxysilane (ICPTES) (Aldrich 95%), ethyl alcohol absolute P.A. (Carlo Erba), tetrahydrofuran P.A. (stabilized - Riedel-de Haën), HCl (ACS Reagent 37% - Sigma-Aldrich), zirconium tetrapropoxide, $\text{Zr}(\text{OPr}^n)_4$ (Aldrich, 70 wt. % in 1-propanol), methacrylic acid (McOH , $\text{CH}_2 = \text{C}(\text{CH}_3)\text{COOH}$, Aldrich, 99%) and butanol (Sigma, 1-butanol, $\geq 99\%$) were used as received. The synthesis of the diureasil host, termed as d-U(600), contains 8.5 (OCH₂CH₂) polymer chains with both ends grafted to a siliceous network by means of urea linkages was recently published [11]. The diureasil d-U(600) was doped with 40% mol of $\text{Zr}(\text{OPr}^n)_4$ with the $\text{Zr}(\text{OPr}^n)_4$:McOH molar ratio of 1:1. The hybrids were processed as thin films deposited on oxidized silicon wafers (with silica thickness of 1 μm). To enable the wafers to be spun, they were held by suction on a chuck, placed on the axis of the spin coater (MIKASA, 1H-DX2) accelerated at 500 rpm for 15 s and 1000 rpm for 30 s. The films were then dried at 50 °C for 12 h, for complete solvent removal. In order to evaluate the performance of both types of optimization by comparing the proximity to the final solution and the appraised reduction of the computation time, we present a comparison between single and multi-objective optimization genetic algorithm considering two films, termed as dUZ40-1 and dUZ40-2, whose ellipsometry data was simultaneously optimized.

2.2. Experimental techniques

The Scanning Electron Microscopy (SEM) images were obtained with a field emission type microscope (JEOL-JSM6335F) operating at 3.0 kV. To reveal the substrate and the film cross section, the samples were cleaved and cleaned with an air flux. The films were fixed on the SEM sample holder with a conductive adhesive. A good image contrast was achieved without the need of any coating process.

The Spectroscopic ellipsometry measurements were made using an AutoSE ellipsometer (HORIBA Scientific) with a total of 250 points in the wavelength interval 440-850 nm, an incidence angle of 70°, an acquisition time of 22 ms per point and an average of 10 measurements per point.

3. Ellipsometry fundamentals

Ellipsometry measures the change in the polarization state of light upon reflection on a sample, in terms of the parameters Ψ and Δ . When linearly polarized light reflects on a surface, there is a shift in the phase ($\Delta = \delta_{rp} - \delta_{rs}$) and a change in the relative amplitude of the parallel (p) and perpendicular (s) components of the electric field ($\tan \Psi = |r_p|/|r_s|$), where r_p and r_s are the complex Fresnel reflection coefficients. The values of the parameters Ψ , and Δ

are related with r_p and r_s by the fundamental equation of ellipsometry: $\tan \Psi e^{i\Delta} = \frac{r_p}{r_s}$. The

overall Fresnel reflection coefficients for a multilayered sample are readily calculated using a matricial method to describe the propagation through each layer [4]. Modern phase modulated ellipsometers measure the parameter values designated as I_s and I_c , being Ψ and Δ calculated using the appropriate formulation, $I_s = \sin(2\Psi)\sin(\Delta)$ and $I_c = \sin(2\Psi)\cos(\Delta)$ [12].

A theoretical model of the sample structure must be employed to calculate I_s and I_c , leaving the parameters of interest (thickness and refractive index) as variables that are obtained, when the calculated ellipsometric data match the experimental one.

The goodness of the fit is generally evaluated with the (unbiased) estimator, the mean squared error (MSE) given by

$$MSE_{IcIs} = \frac{1}{2N - M - 1} \sum_{j=1}^N \left\{ \left(I_{c_j}^{\text{mod}} - I_{c_j}^{\text{exp}} \right)^2 + \left(I_{s_j}^{\text{mod}} - I_{s_j}^{\text{exp}} \right)^2 \right\} \quad (1)$$

where N is the number of experimental data, M is the number of the model variable parameters, and the subscripts *exp* and *mod* stands for the measured and simulated data, respectively.

The optical constants for the film were calculated using the Lorentz model, which expresses the relative complex dielectric constant as a function of the frequency ω (eV), described by

$$\varepsilon = \varepsilon_{\infty} + \frac{(\varepsilon_s - \varepsilon_{\infty})\omega_0^2}{(\omega_0^2 - \omega^2) + i\Gamma\omega} \quad (2)$$

where ε_{∞} , ε_s , ω_0 (eV), Γ (eV) are the high frequency relative dielectric constant, the static relative dielectric constant, the oscillator resonant frequency and the damping factor, respectively.

This model does not take into account all the resonant transitions, being limited in terms of application range. However, for a restrict wavelength range (as in the present case) this model is adequate to describe the relative complex dielectric function of the films.

4. Multi-objective optimization

Two of the commonest approaches with multi-objective optimization problems are to combine the individual objective functions into a single composite function or to determine a set of Pareto optimal solutions. For the first approach the weights assigned to each normalized objective function, converts the problem into a single objective one [13]. In the later approach a set of solutions that are non-dominated or superior with respect to each other, is determined [13]. For a given set of functions z_i with $i = 1, \dots, k$, a point x is said to dominate another point y ($x > y$) only if $z_i(x) \leq z_i(y)$ for $i = 1, \dots, k$ and $z_j(x) < z_j(y)$ for at least one objective function j [13]. The solutions which are non-dominated by any other belong to the so called Pareto set. The corresponding objective function values in the objective space are termed as Pareto front.

To describe the application of multi-objective optimization in ellipsometric data analysis, we considered the combination of measurements for two films. Using conventional optimization for the data analysis, the MSE value for each film is combined in the one objective function simply by summation or weighted summation. With multiple objective optimization for each film k an objective function ($MSE_{IcIs,k}$) is built. The same principle is valid for films that are measured at different positions or when measurements are performed at different angles of incidence. Another possibility is the application in cases where external data is available, assigning one objective function to ellipsometric data and the other, for example, to reflectance data.

For complex problems MOGA extends the advantages of GA because it takes into consideration the individual fitness of each function, finding multiple non-dominated solutions. Therefore, the quality and uniqueness of MOGA solutions are, in principle, superior to those provided by single objective optimization. It is important to note that evolutionary algorithms that use the non domination sorting (NDS) are not suited for problems with more than four objective functions. This is due to the fact that a major number of initially generated solutions will be actually non-dominated, which makes difficult to guide the search. These problems are tackled with many-objective optimization algorithms [13].

Among the various MOGA's, one of the most popular, due to the good overall efficiency and easiness to implement, is a NSGA II (Non Dominated Sort Genetic Algorithm) based algorithm [14]. Originally this algorithm is bi-objective but it can readily be extended for more functions.

It is useful to implement a method for constraint handling, whenever it is possible. We have implemented a procedure in which every new individual, generated by simulated binary crossover (SBX) [15] or polynomial mutation [15], is checked to verify if all chromosomes

are in the feasible region. An infeasible chromosome is replaced with one resultant of an arithmetic crossover of the two parents. Common methods for GA's constraints handling are based on penalty functions, which takes in account the feasibility of the solutions in the fitness values of the individuals. Our strategy simply relies on the working principle of genetic algorithms, if the repaired solution has poor fitness it will be naturally rejected.

Seeking the comparison between single and multi-objective optimization, we implemented a single objective genetic algorithm, termed as common genetic algorithm (CGA), which uses the same crossover and mutation operator than the MOGA, and the traditional tournament selection. Nor NDS nor crowding distance comparison is used. Therefore both algorithms are identical and the same building blocks are used, enabling a fair comparison of the results. The control parameter of SBX is 20 and polynomial mutation is 20 both for MOGA and CGA and the number of individuals generated by crossover, for both algorithms, is equal to the population size. The implemented single objective LO method was the Interior-Point algorithm with Hessian calculated by Broyden–Fletcher–Goldfarb–Shanno quasi-Newton approximation. The initial point for the LO method is the best solution found by the GA. The minimization algorithms were implemented in MATLAB®.

5. Example of the multi-objective optimization testing

Figure 1(a) shows an SEM image of a dUZ40 film, revealing that the di-ureasil layer prepared by spin-coating has a uniform crack-pinhole-free dense microstructure with an average thickness of $0.835 \pm 0.028 \mu\text{m}$. Based on this layered structure the model structure scheme for the dUZ40 planar waveguides in Fig. 1(b) will be considered in the ellipsometric data analysis. The surface roughness was previously studied by atomic force microscopy, revealing low root-mean-square roughness values ($<1 \text{ nm}$) [10]. Therefore, no surface roughness layer was considered in the structure model.

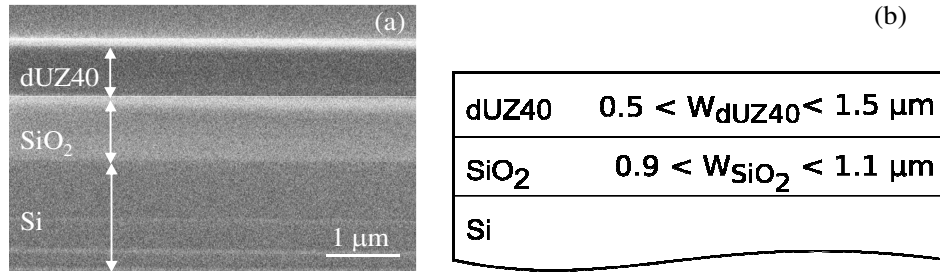


Fig. 1. (a) SEM photo of the cross-section and (b) structure model of the dUZ40 planar waveguides.

Figure 2 displays the experimental ellipsometric parameters I_s and I_c measured for the dUZ40-1 and dUZ40-2 planar waveguides. For comparison purposes the fitting for parameters extraction was implemented with two minimization algorithms (MOGA/LO and CGA/LO). The fitting parameters for each sample are the layers thickness (W_{SiO_2} and W_{UZ40} , Fig. 1(b)) and the parameters related with the material relative complex dielectric constant are assumed to be equal for the two dUZ40. For the silicon and silica layers reference values for the refractive index were utilized [16]. We have chosen very broad variation intervals for the initial bounds for the individual (W_{SiO_2} and W_{dUZ40} , Fig. 1(b)) and for the shared parameters (ϵ_∞ , [0.00,3.00], ϵ_s , [0.05,3.00], ω_0 [5.0,20.0] and Γ , [0.0,1.0]), in order not to introduce any bias in the final value. The optimization process was realized using 500 generation and a population size of 1000 individual for both GO's, increasing by this way the probability that the final solution corresponds to the global minimum. Both algorithms converge to the same final values with a variation between iterations smaller than 10^{-15} and a MSE value of 1.52×10^{-3} , Fig. 2.

The final solution determined with MOGA/LO and CGA/LO yielding to $1.0220 \pm 0.0009 \mu\text{m}$ and $1.0219 \pm 0.0009 \mu\text{m}$ for W_{SiO_2} and $0.7948 \pm 0.0006 \mu\text{m}$ and $0.7924 \pm 0.0012 \mu\text{m}$ for

W_{UZ40} , respectively, for the two planar waveguides (Table 1). These values are in good agreement with the thickness values commercially available for the buffer layer of SiO_2 and with the organic-inorganic layer thickness estimated by SEM images (Fig. 1(a)). The attained refractive index values for the planar waveguides were 1.5111 ± 0.0010 and 1.5055 ± 0.0007 for a wavelength of 535 nm and 632.8 nm, respectively. These results are in good agreement with those previously reported for analogous di-ureasil planar waveguides [9,17]. The final ϵ_∞ value is smaller than 1, which results from the fact that the used model does not take into account all the resonant transitions. Therefore, this value cannot be taken as the permittivity value at high frequencies but only a fitting parameter for the analyzed wavelength interval.

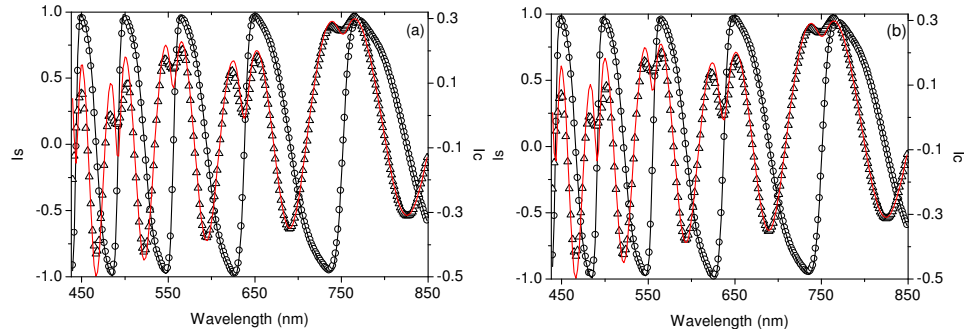


Fig. 2. Ellipsometric parameters I_s (open circles) and I_c (open triangles) for (a) dUZ40-1 and (b) d-UZ40-2. The solid lines correspond to the data best fit ($\text{MSE} = 1.52002 \times 10^{-3}$).

Table 1. Individual (thickness for the SiO_2 , W_{SiO_2} and dUZ40, W_{dUZ40} layers) and shared (high frequency relative dielectric constant, ϵ_∞ , static relative dielectric constant, ϵ_s , oscillator resonant frequency, ω_0 , and damping factor, Γ) parameter values determined using MOGA/LO and CGA/LO algorithms for dUZ40 films.

Individual parameters			Shared parameters			
Material	W_{SiO_2} (μm)	W_{dUZ40} (μm)	ϵ_∞	ϵ_s	ω_0 (eV)	Γ (eV)
dUZ40-1	1.0220 ± 0.0009	0.7948 ± 0.0006	0.80 ± 0.04	2.2264 ± 0.0002	11.8 ± 0.2	0.2522 ± 0.0003
dUZ40-2	1.0219 ± 0.0009	0.792 ± 0.001				

The relevant question to optimize the minimization procedure is to decide the right moment to switch from GA to LO. To improve the GA search, it is necessary to properly dimension the population size, the initial range and the number of generations.

To quantify the MOGA and CGA algorithms performance Fig. 3(a) shows the Euclidean distance from the solution obtained after the application of GA to the one achieved after the LO optimization, as function of the generation number. In this analyze it was considered a population of 400 elements, being the final value the average of 50 runs, with the standard deviations represented as errors bars. Since GA's are stochastic optimizers, there is a natural randomness associated with the presented results, thus they should be taken as indicative of a trend. The Euclidean distance to the final solution is clearly dependent on the number of generations, being also clear that the proposed MOGA algorithm produces results with a distance to the final solution smaller than the CGA and with low dispersion around the average value of the 50 runs. It is also noticeable that the MOGA Euclidean distance displays a decay behavior with the number of generations and, consequently, presents an asymptotic behavior as the number of generations unlimitedly increases. Thus, we can conclude that it is not worthwhile the unlimited increase in the number of generations to improving the method's accuracy.

A good choice for the initial population values in the LO algorithm is very important, because the next generations are framed upon the best members of the previous generation. Therefore, the best initial population value was studied. For the case of 20 and 200

generations, and for several population sizes we applied the LO to the best solution of each one of the 50 runs. The termination conditions for the local optimizer were that the MSE had a value smaller than 1.5201×10^{-3} and a variation between iterations smaller than 10^{-15} . Figure 3(b) shows the percentage of convergence successes in 50 trials taken by the local optimizer to converge. It is clear that for higher population sizes, even when the algorithm is switched at a higher MSE value (20 generations) the LO method is almost able to reach a desirable minimum. However, MOGA reaches the optimization minimum value for a lower population size with lower computational effort.

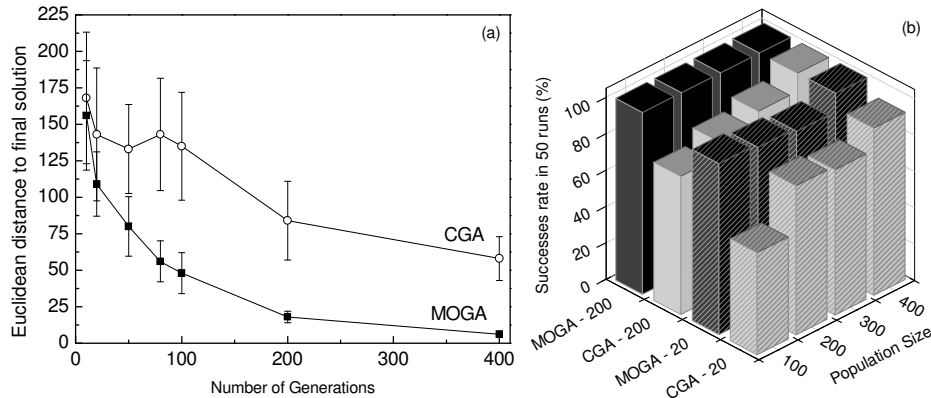


Fig. 3. (a) Euclidean distance to the final solution (50 runs and population of 400 elements) as function of the generation's number for CGA and MOGA algorithms (population size of 400 individuals). The lines are visual guides. (b) Convergence rate for 50 iterations as function of the population size for the two considered algorithms.

The results make clear that, even being GA's stochastic optimizers; there is a trend in it that indicates a better performance from multi objective than the one found in common genetic algorithms. The explorative capacity of GA's makes this type of optimization well suited to address problems with many variables and large search spaces.

The difference in performance of both algorithms could be explained regarding the non dominated solutions. The MOGA solutions that are simultaneously better for both samples are preferred to evolve, while the CGA ones with higher probability to evolve correspond to the better fitness for the sum of all solutions (independently of each individual fitness).

6. Conclusions

We have introduced for the first time the use of hybrid multi-objective optimization in spectroscopic ellipsometry data analysis. The procedure was validated, using planar waveguides of sol-gel derived organic-inorganic hybrids on oxidized silicon wafers. For the implementation of the hybrid optimization a single objective common genetic algorithm (CGA) was compared to a multi-objective genetic algorithm (MOGA), showing a higher success rate in the task of finding the best final solution for MOGA. Furthermore, we demonstrated that the hybrid MOGA is potentially faster than the CGA and also that its efficiency can be improved when the right moment to switch methods is properly chosen.

Acknowledgments

Funding was provided by Fundação para a Ciência e a Tecnologia, FEDER (PTDC/CTM/72093/2006, SFRH/BD/41943/2007) and COST Action MP0702. The authors also thank E. Pecoraro from Instituto de Telecomunicações, University of Aveiro, for help in the hybrids' synthesis.